

SYNOVIUM-DERIVED STROMAL CELL-INDUCED OSTEOCLASTOGENESIS: A POTENTIAL OSTEOARTHRITIS TRIGGER.

Manuela Dicarlo, PhD^{1*}, Gabriella Teti, PhD^{2*}, Giorgia Cerqueni, BS³, Iolanda Iezzi, MD³, Antonio Gigante, MD³, Mirella Falconi, MD², Monica Mattioli-Belmonte, PhD^{3#}

*Both Authors Equally contributed to the Research

¹ Laboratory of Experimental Immunopathology, IRRCs “S de Bellis”, Castellana Grotte, 70013, Bari, Italy

² Department of Biomedical and Neuromotor Sciences-DBNS, Università di Bologna, Via Irnerio 48, 40126 Bologna, Italy.

³ Department of Clinical and Molecular Sciences (DISCLIMO), Università Politecnica delle Marche, 60126, Ancona, Italy [#]Correspondence to: m.mattioli@univpm.it

Running title: Synovium Stromal Cells as osteoarthritis trigger

Keywords: Synovium-Derived Stromal Cells, Osteoarthritis, Telocytes, osteoclastogenesis

Acknowledgments: The authors are grateful to Dr. Andreil Hossein for her English revision. This study was funded by grants of the Università Politecnica delle Marche to Prof. Monica Mattioli-Belmonte. No benefits in any form have been, or will be, received from a commercial party directly, or indirectly, related to the subject of this article.

Statement of author contributions:

Prof. Mattioli-Belmonte planned and oversaw the whole research; Prof. Gigante furnished tissue samples and clinical suggestion; Dr. Dicarlo executed cell cultures; Dr. Cerqueni performed immunohistochemical analysis; Prof. Teti was responsible for ultrastructural investigation; Dr. Iezzi was responsible for qRT-PCR analysis; Prof. Falconi oversaw morphological analyses. All authors equally and competently contributed to the draft.

Conflict of interest statement: The authors declare that they have no conflict of interest.

1 **Abstract**

2 **Purpose:** To shed light on the idea that mesenchymal stem/stromal cells recruited in synovium
3 (Synovium-Derived Stromal Cells-SDSCs) could be involved in Osteoarthritis (OA)
4 pathophysiology. Attention was also paid to a further stromal cell type with a peculiar
5 ultrastructure called telocytes (TCs), whose role is far to be clarified. **Methods:** In the present *in*
6 *vitro* study we compared SDSCs isolated from healthy and OA subjects in terms of phenotype,
7 morphology and differentiation potential as well as in their capability to activate normal Peripheral
8 Blood Mononuclear Cells (PBMCs). Histological, immunohistochemical and ultrastructural
9 analyses were integrated by qRT-PCR and functional resorbing assays. **Results:** Our data
10 demonstrated that both SDSC populations stimulated the formation of osteoclasts from PBMCs:
11 the osteoclast-like cells generated by healthy-SDSCs via trans-well co-cultures were inactive, whilst
12 OA-derived SDSCs have a much greater effectiveness. Moreover, the presence of TCs was more
13 evident in cultures obtained from OA subjects and suggests a possible involvement of these cells in
14 OA. **Conclusions:** Osteoclastogenic differentiation capability of PBMCs from OA subjects, also
15 induced by B synoviocytes has been already documented. Here we hypothesized that SDSCs,
16 generally considered for their regenerative potential in cartilage lesions, have also a role in the
17 onset/maintenance of OA. **Clinical Relevance:** Our observations may represent an interesting
18 opportunity for the development of a holistic approach for OA treatment, that considers the
19 multifaceted capability of MSCs in relation to the environment.

20

21 **Clinical Perspectives summary**

22

23 **1. Background:** Mesenchymal stem/stromal cells recruited in synovium (Synovium-Derived
24 Stromal Cells-SDSCs), generally considered for their regenerative potential in cartilage
25 lesions, could have a role in the onset/maintenance of OA. Telocytes (TCs) were also
26 investigated.

27 **2. Results:** Our in vitro study showed that only the SDSCs harvested from OA subjects were
28 capable to generate active osteoclasts from healthy donor PBMCs. TCs were more
29 numerous in cultures obtained from OA in comparison to healthy subjects, suggesting their
30 possible involvement in OA.

31 **3. Potential significance:** Cartilage regeneration strategies in OA must take into account the
32 multifaceted capability of MSCs in relation to the environment.

33

34

35 **1. Introduction**

36 Osteochondral defects may progress in osteoarthritis (OA), which is one of the most common
37 sources of articular pain and disability in an aging population [1]. To date, several therapeutic
38 efforts have been made, but no treatment has been proven to stabilize, reverse or prevent OA
39 development, and cartilage recovery continues to represent a challenge to scientists and clinicians
40 [2]. OA is currently defined as a disease of the whole joint, as it affects not only the cartilage but
41 also the subchondral bone and the synovial tissue [3]. Recent researches are focusing on an in-depth
42 characterisation of cells harvested from the synovium (SM) of normal and OA subjects to elucidate
43 their involvement in the regeneration and/or pathogenesis of joint diseases.

44 SM is a specialized mesenchymal tissue that includes two layers: the intima in contact with
45 the articular cavity, which is composed of one or two cell sheets, and the underlying subintima,
46 consisting of abundant collagenous extracellular matrix (ECM) with dispersed fibroblast-like cells,
47 macrophages, mast cells, autonomic nerve fibers, and blood and lymphatic vessels [4,5]. The
48 intima encompasses two morphologically different cell types named Type A and Type B
49 synoviocytes. The former are bone marrow-derived phagocytic cells participating in the clearance
50 of debris from the joint cavity and serving as immune sentinels. Type B synoviocytes, a kind of
51 mesenchymal cells, are responsible for the production of synovial fluid molecular components,
52 including hyaluronan and lubricin [4,5]. The subintima consists of a loosely organized and highly
53 vascularized connective tissue that forms a support for the overlying intima [4–6]. It allows the
54 transfer of molecular and cellular components from the circulation to the intima and synovial fluid
55 in the articular cavity [7] and represents a potential reserve of type B synoviocytes for the
56 maintenance of synovial intima integrity [7]. The subintima contains also immune competent cells.

57 Human SM hosts Mesenchymal Stromal Cells (MSCs) [8,9], called Synovial-Derived Stem
58 Cells (SDSCs), that share the same phenotypic and functional properties of bone marrow (BM)
59 MSCs [10]. Identification of MSCs in the synovium has raised speculations about their biological

60 involvement in the normal or pathologic joint physiology. Their possible role in synovial intima is
61 related to their potential to differentiate into a wide variety of diarthrodial joint cell types (i.e.
62 chondroblasts, osteoblasts and adipocytes). SDSCs were shown to have the greatest chondrogenesis
63 potential among the mesenchymal tissue-derived cells, representing a possible source for cartilage
64 repair [11]. SDSCs were also demonstrated to be superior in terms of adipogenesis [12] and,
65 together with those of periosteum, were shown to be superior in osteogenesis [13,14]. These results
66 indicate the therapeutic potential of SDSCs for the treatment of chondral defects. SDSCs can be
67 found both in healthy and OA cartilage [11,13], and unlike BM MSCs, SDSCs seem to maintain an
68 efficient proliferation rate and colony-forming potential regardless of the age of the patient [15].
69 Furthermore, these cells may be involved in early stages of osteoarticular diseases [16]. Recently, the
70 presence of a further stromal cell type with a peculiar ultrastructure called telocytes (TCs) has also
71 been described in various human tissues including SM [17]. TCs possess very long and thin cellular
72 extensions (telopodes) constituted by a repetition of thin segments (podomeres) and dilated portions
73 (podoms) [18]. Their role is far to be clarified both in terms of tissue regeneration and disease
74 occurrence.

75 Even if there are studies demonstrating the production of osteoclastogenic factors by synovial cells,
76 not enough findings support the hypothesis that SDSCs could be implicated in OA
77 pathophysiology. The purpose of our study was to isolate and culture SDSCs from healthy and OA
78 SM and compare in vitro differences in term of morphology, phenotype, differentiation potential
79 and capability to activate normal Peripheral Blood Mononuclear Cells (PBMCs).

80

81 **2. Materials and Methods**

82 **2.1 Synovium (SM) and Synovial-Derived Stem Cells (SDSCs) isolation**

83 SM was obtained during surgery for total knee arthroplasty in eight OA subjects (mean age 86 ± 3),
84 treated in the Azienda Ospedaliera-Universitaria Ospedali Riuniti of Ancona (Italy) from January
85 2015 to April 2017. Control SM was obtained from 2 healthy subjects, gender matching,

86 undergoing leg amputation. In accordance with the Local Ethical Committee guidelines and with
87 the 1964 Helsinki declaration an informed consent was obtained from all individual participants
88 included in the study. Patients were aware that the tissue used for the study represented a discard of
89 surgical procedures and the voluntariness of their participation to the study (freedom from coercion
90 or undue influence, real or imagined). SDSCs were isolated according to De Bari et al [8]: briefly,
91 synovial tissues were rinsed with Dulbecco's Phosphate Buffered saline (DPBS) (Sigma-Aldrich,
92 Milan, Italy), minced into small pieces and then digested with 0.2% collagenase (Collagenase NB
93 4G Proved Grade, Serva Electrophoresis GmbH, Germany) in Dulbecco's Modified Eagle
94 Medium/Nutrient Mixture F-12 (DMEM/F-12, Sigma-Aldrich), supplemented with 2% Foetal
95 Bovine Serum (FBS) and 1% penicillin-streptomycin (100U/ml) at 37°C in a humidified atmosphere,
96 with 5% CO₂. FBS and antibiotics were both from GIBCO® (Thermo Fisher Scientific, Waltham,
97 MA, USA). After an overnight incubation, samples were filtered through 40µm nylon-mesh cell-
98 strainers (BD Biosciences, San Jose, CA) to remove large debris. Single cell suspensions were
99 cultured in DMEM/F-12 with 10% FBS and 1% antibiotics (from here on defined Complete
100 Medium-CM) in tissue culture flasks, changing CM twice a week. Upon reaching 50% confluence,
101 cells were carefully detached with 0.25% trypsin/1mM EDTA (Sigma-Aldrich). Non-adherent cells
102 were gradually lost by medium changing. From each explant we were able to obtain an adequate
103 number of cells without excessive subculturing (i.e. within the 4th passage of subculture) allowing
104 the set up two different sets of experiments.

105

106 **2.2 SDSCs Characterization**

107 Immunophenotype of synovial adherent cells was investigated by flow cytometry according to the
108 minimal criteria of the International Society for Cellular Therapy (ISCT) [19]. The following
109 fluorescein isothiocyanate (FITC)-conjugated mouse monoclonal antibodies (all by Immunotools,
110 Friesoythe, Germany) were used: anti-CD14 (Clone MEM-15), CD34 (Clone 4H11-APG), CD45
111 (Clone MEM-28), CD73 (AD2), CD90 (Clone 5E10, StemCell Technologies, Milan, Italy), CD105

112 (Clone MEM-226) and CD106 (Clone STA). As isotype controls, FITC-coupled nonspecific mouse
113 IgG replaced the primary antibodies. For each sample, at least 10,000 events were acquired by
114 FACSCalibur flow cytometry system (Becton Dickinson, CA, USA) and data were analysed using
115 FCS Express 6 Plus Software (De Novo Software, CA, USA). Forward (FSC) monitored the cell
116 volume and Side scatter (SSC) evaluated the internal complexity.

117

118 **2.3 SDSCs in vitro differentiation**

119 For in vitro chondrogenic, osteogenic and adipogenic differentiation, commercial kits from Life
120 Technologies Corporation (Carlsbad, USA) were used according to manufacturer's instructions.

121 For in vitro, chondrogenic, osteogenic and adipogenic differentiation commercial kits from Life
122 Technologies Corporation (Carlsbad, USA) were used according to manufacturer's instruction (for
123 details see supplementary information). The chondrogenic potential of adherent cells isolated from
124 synovia was assessed using a pellet culture system. In brief, 5×10^5 cells were centrifuged for 10
125 minutes (min) in 15 mL polypropylene tubes and then cultured for 14 days in 1mL of STEMPRO®
126 chondrogenic medium (Chondrogenesis Kit, Life Technologies Corporation, USA), replacing
127 medium every 3–4 days. Cell pellets were paraffin-embedded, cut into 3 μ m thick sections, and then
128 stained with Alcian Blue solution pH 1 (Bio-Optica, Milan, Italy). For immunohistochemistry,
129 deparaffinized sections were incubated with mouse monoclonal antibodies against aggrecan (Clone
130 3H524, dil. 1:20, Santa-Cruz Biotechnology inc, Heidelberg, Germany) and type II collagen (Clone
131 II-4C11, dil 1:10, Merck Millipore, Darmstadt, Germany). After overnight incubation at 4°C, the
132 immune complex was evidenced by the streptavidin–biotin peroxidase technique (Envision
133 peroxidase kit, DakoCytomation, Milan, Italy). After the incubation with 0.05% 3,3'-
134 diaminobenzidine (Sigma-Aldrich) in 0.05M Tris buffer, pH 7.6 with 0.01% hydrogen peroxide,
135 samples were counterstained with Mayer's haematoxylin (BioOptica) dehydrated in ethanol and
136 coverslipped with Eukitt mounting medium (Electron Microscopy Sciences, PA, USA).

137 For osteogenesis, cells were seeded in chamber slides (Nunc™, Rochester, NY) at a density of 5 x
138 10³ cells cm⁻² in appropriate induction medium (STEMPRO® Osteogenesis Kit, Life
139 Technologies). After 21 days, Von Kossa staining evaluated matrix mineralization.

140 Adipogenic differentiation was performed by culturing 2 x 10⁴ cells cm⁻² with STEMPRO®
141 Adipogenesis Kit (Life Technologies) for 14 days and detected by Oil Red staining (Sigma-Aldrich)
142 according to manufacturer's instruction. The appearance of cytoplasmic lipid droplets was also
143 identified by immunohistochemistry using a mouse antibody against perilipin 1 (dil. 1:100; Abcam,
144 Cambridge, UK) and evidenced as described above.

145 Cells maintained in CM represented the negative controls. Nikon DSVi1 digital camera and NIS
146 Elements BR 3.22 imaging software (both from Nikon Instruments, Florence, Italy) were used for
147 images acquisition.

148 **2.4 Ultrastructural analysis**

149 For Transmission Electron Microscopy (TEM), tissue and cells were fixed in 2.5% glutaraldehyde
150 in 0.1 M cacodylate buffer for 2 h at 4°C, post-fixed in 1% Osmium tetroxide in 0.1 M cacodylate
151 buffer for 30 min at Room temperature (RT), dehydrated in an acetone series (70%, 90% and 100%)
152 and embedded in Epon resin (Fluka, Sigma-Aldrich). 100 nm ultra-thin sections were cut using a
153 Diatome diamond knife (Diatome, Hatfield, PA, USA) on a Reichert-Jung ultramicrotome (Ultracut
154 E, Reichert G, Wien, Austria). Sections were picked up on nickel grids and stained with alcoholic
155 uranyl acetate and Reynold's lead citrate. Ultrastructural examination was performed using the
156 Philips CM10 Transmission Microscope equipped with Megaview III digital camera (FEI
157 Company, Eindhoven, The Netherlands).

158 For Scanning Electron Microscopy (SEM) cells were fixed as described above, dehydrated in
159 increasing ethanol concentrations (25%, 50%, 70%, 80%, 95% and 100%), dried by evaporation of
160 hexamethyldisilazane (HMDS), mounted on aluminium stubs, gold-sputtered and observed with a
161 SEM Philips XL 20 (FEI, Milan Italy).

162

163 **2.5 Osteoclastogenesis**

164 In vitro osteoclastogenesis was induced in Peripheral Blood Mononuclear Cells (PBMCs) by
165 SDSCs through a Transwell (Thermo Scientific™ Nunc™ Carrier Plate system, Milan, Italy) co-
166 culture system. PBMCs were obtained from gender matching healthy donors using density gradient
167 Ficoll/Paque method. In brief, peripheral blood was diluted 1:1 in DPBS, layered on Histopaque®-
168 1077 (Sigma-Aldrich) and centrifuged at 400g for 30 min. PBMCs at the interface plasma/Ficoll
169 were collected, washed in DPBS, suspended in α -MEM (Corning Inc., NY, USA) supplemented
170 with 20% FBS, 1% antibiotics and 2 ng/mL of M-CSF (PeproTech EC, London, UK). Cells were
171 then seeded at a density of 2×10^6 cells/well on Aclar® Film 33C (EMS, Fort Washington, PA,
172 USA) placed in a 12 wells tissue culture plates (TCPs). Cells were cultured for 6 days, removing
173 non-adherent cells with media changes. SDSCs were then seeded in cell culture inserts (with pores
174 $0.4 \mu\text{m}$) of the 12 wells TCPs containing PBMCs, at a density of 2×10^5 cells/well (ratio 1:10). Co-
175 cultures were maintained for 2 weeks. At each culture media refresh, adherent cells were observed
176 by a light inverted microscope to assess multinucleated cell development. After 14 days, the inserts
177 were removed, and cells in the wells analysed for cytoskeleton distribution and the IHC expression
178 of Tartrate-resistant acid phosphatase (TRAP) and cathepsin K (CTSK). For methodological details
179 see Supplementary Information (SI1). TRAP- or CTSK- positive multinuclear cells that contained
180 more than three nuclei were identified as osteoclasts and counted. Nikon DSVi1 digital camera and
181 NIS Elements BR 3.22 imaging software were used for images acquisition.

182 For the immunostaining evaluation of TRAP and Cathepsin K four images at 20X magnification
183 from each sample were analyzed in semi-quantitative manner. For each image, cells with more than
184 3 nuclei were examined for TRAP and CatK staining and ranked as: 0 (negative), 1 (weak staining),
185 2 (good staining), 3 (strong staining). The score was calculated considering the number of positive
186 cells and the staining rank, and analysed by GraphPad PRISM 4
187 (<https://www.graphpad.com/scientific-software/prism/>).

188 The resorptive ability of generated osteoclasts was assessed putting dentine discs (1 cm in diameter
189 and 0.7 µm in thickness) at the bottom of the wells of the previously described co-culture systems
190 and observed with a SEM Philips XL 20.

191

192 **2.6 qRT-PCR**

193 The expression of genes involved in osteoclastogenesis (Interleukin 6 - IL-6, Receptor activator of
194 nuclear factor kappa-B ligand - RANKL and osteoprotegerin - OPG) was assessed in SDSCs before
195 and after co-culture with PBMCs. Total RNA was extracted from cell pellets using the PerfectPure
196 RNA cultured cell kit (5-Prime GmbH, Hamburg, Germany) according to the manufacturer's
197 instructions. RNA quantity and quality were evaluated by UV spectrophotometric analysis
198 (bioPhotometer plus, Eppendorf GmbH, Germany). Standard reverse transcription was performed
199 using the GoScript™ reverse transcription system (Promega Corporation, Italy) starting from
200 1.0µg of total RNA. Each real-time quantitative PCR assay was executed in triplicate in white
201 plastic ware using the Mastercycler Realplex2 (Eppendorf GmbH). A final volume of 10µl with
202 1µL of cDNA (corresponding to 50 ng of total RNA template), 1X SsoFast™ EvaGreen®
203 Supermix (Bio-Rad), and 200nM primers were used for PCR. The cycling conditions included an
204 initial step at 95 °C for 30 s, followed by 40 cycles at 95°C for 5s and at 60°C for 20s.

205 Oligonucleotide sequences were designed with Primer 3 (v. 0.4.0) software: Interleukin (IL)-6
206 (Forward: CCAGAGCTGTGCAGATGAGT; Reverse: CATTGTGGTTGGGTCAGGG),
207 Osteoprotegerin - OPG (Forward: TGATGGAAAGCTTACCGGGA; Reverse
208 CAGGATCTGGTCACTGGGTT); Receptor Activator of Nuclear Factor κB ligand – RANKL
209 (Forward: TAATGCCACCGACATCCCAT; Reverse; ATGTTGGAGATCTTGGCCCA). To avoid
210 sequence homologies to pseudogenes or other undesired targets, primer specificity was checked by
211 BLAST. Melt curve analysis confirmed PCR specificity. Reference genes and each gene of interest
212 were amplified simultaneously under the same conditions in each PCR assay. Primers showed the
213 same amplification efficiency. Glyceraldehyde 3-phosphate dehydrogenase – GAPDH (Forward:

214 AGCCACATCGCTCAGACAC; Reverse: GCCCAATACGACCAAATCC) and beta-
215 glucuronidase – GUSB (Forward: AAACGATTGCAGGGTTTCAC; Reverse
216 TCTCGTCGGTGACTIONGTTCA) were used to normalize cellular mRNA data [20]. Normalization
217 involved the ratio of mRNA concentrations of genes of interest (Ct values) to that of reference gene
218 Ct medium values. Data were expressed as relative gene expression ($2^{-\Delta Ct}$). Each assay was
219 performed in triplicate. To point out the effect of the different origin (OA vs H) or the co-culture
220 system on SDSCs, $\Delta\Delta Ct$ method for Fold-Change evaluation was used [21]. The qPCR efficiency
221 in all our experiments was more than 90%.

222

223 **2.7 Statistical analysis**

224 Statistical analysis was performed by Prisma 4 Software ([https://www.graphpad.com/scientific-
225 software/prism/](https://www.graphpad.com/scientific-software/prism/)). Mean and standard deviation of two different experiments for cells obtained from
226 each subject were analyzed by Mann–Whitney U test. Statistical significance was tested at $p <$
227 0.05.

228

229 **3. Results**

230 **3.1 Synovium**

231 Semithin sections of OA and healthy SM were subjected to toluidine blue staining to examine their
232 general morphological features, followed by ultrastructural analysis of ultrathin sections to
233 investigate the presence TCs. Cells with long and thin cytoplasmic processes were observed in
234 toluidine blue-stained synovial semithin sections.

235 TEM observation evidenced the presence of Type B synoviocytes, characterized by a large body
236 rich in mitochondria and cisternae of rough endoplasmic reticulum (RER), a large Golgi apparatus
237 and short and thick processes. Synovial TCs generally showed a relatively large and slightly
238 indented euchromatic nucleus, with patches of heterochromatin near the nuclear membrane. The
239 cytoplasm contained few mitochondria, few RER cisternae and a small Golgi apparatus. Telopodes,

240 with a narrow emergence from the cellular body, were also evident. They displayed a repetition of
241 extremely slim segments (podomers) and expanded parts (podoms) with RER and mitochondria. In
242 OA-SM, mastocytes were also evident (Figure 1).

243

244 **3.2 SDSCs characterization and differentiation ability**

245 No differences in the phenotypic expression of common MSC markers were detected between
246 SDSCs isolated from Synovium of OA and healthy subjects. Cells were positive for CD73, CD90
247 and CD105 (>98% of positive cells), whilst they were negative for hemopoietic antigens CD14,
248 CD34 and CD45 (positivity <2%) (Fig. 2a). On the contrary, significant differences between
249 healthy and OA cells were detected for the expression of CD106 ($42.75\pm 2.14\%$ vs $49.02\pm 2.45\%$;
250 $p<0.05$).

251 The analysis of cell size (FSC) and internal granularity (SCC) revealed that SDSCs obtained from
252 OA subjects were significantly larger than the healthy counterpart (250.49 ± 6.89 vs 216.98 ± 12.77 ,
253 $p<0.01$) and showed an increased internal complexity (385.32 ± 10.77 vs 339.20 ± 8.13 , $p<0.01$).

254 No changes in the cell differentiation potential of healthy and OA SDSCs were detected (Fig 2b) as
255 underlined by the comparable Alcian Blue staining and immunohistochemical expression of
256 aggrecan, Von Kossa and Alizarin Red mineralization assays, and Oil Red O-staining and perilipin
257 immunohistochemical expression (Fig. 2b).

258

259 **3.3 SDSC ultrastructure**

260 SEM observation showed the presence of cells with different morphologies. In healthy- derived
261 cells both Synoviocytes A and B were detectable. Some SDSCs showed oligodendritic (2-3
262 extended cell processes) and polydendritic (more than 4 cell processes). This morphology was
263 suggestive for TCs. TEM analysis corroborated SEM observation even if cell monolayer hampered
264 the correct visualization of telopodes (Fig. 2c).

265

266

267

268 **3.4 Osteoclastogenesis**

269 No evident multinucleated cells were observed until day 8 of SDSCs/PBMC co-culture. After 3
270 days of co-culture, adherent cells in the lower wells consisted of a mixed population of fibroblast-
271 like and round shaped cells. From day 8, several multinucleated cells appeared in both OA SDSCs
272 and healthy co-culture systems (Fig. 3a). After 14 days, F-actin ring formation and cytoskeletal
273 tubulin revealed the presence of plentiful F-actin ring positive cells containing more than 3 nuclei in
274 both samples and zipper-like structures (Fig. 3a).

275 At 14 days multinucleated cells were positive for TRAP and CTSK in both OA co-culture and
276 healthy system, with several TRAP⁺ cells showing a slight albeit not significantly increase in OA
277 SDSCs co-culture system. On the contrary, a decrease in the number of the CTSK⁺ was observed
278 (Figure 3b). The presence of multinucleated cells and resorbing pits were confirmed by SEM
279 observation of osteoclast-like cells induced by OA-SDSCs (Fig 3c).

280

281 **3.5 qRT-PCR**

282 The relative expressions of IL-6 (4-fold) and OPG (2-fold) were down-regulated in SDSCs
283 harvested from OA-subjects in comparison with H-SDSCs (Table 1). On the contrary, RANKL
284 mRNA evidenced a significant increase, which was further responsible for the increase of
285 RANKL/OPG ratio in OA-SDSCs.

286 The mRNA expression of OPG and RANKL was evaluated in SDSCs also after co-culture (Table
287 1). The comparison with their expression before and after co-culture evidenced an up-regulation of
288 RANKL mRNA expression in H-SDSCs (8-fold) and a slight albeit significant decrease in OA-
289 SDSCs. A different behavior was detected for OPG mRNA that was up-regulated in both SDSCs
290 after co-culture. These changes resulted in significantly higher RANKL/OPG ratio in H-SDSCs in
291 comparison to OA cells (Fig.3).

292

293

294 **4. Discussion**

295 Osteoarthritis (OA) is the most common form of chronic joint disease, representing the leading
296 cause of pain and disability in an aging population. Despite its association with the aging process
297 [22], at present OA is recognized as a pathology of the whole joint, including closely related
298 changes in cartilage, synovium and subchondral bone [23]. The synovium entails the synovial
299 membrane, which encapsulates the joint providing structural support, synovial fluid for proper
300 lubrication and nutrients essential for normal joint function [4]. The subchondral region consists of
301 the cortical bone underlying the calcified cartilage (subchondral plate) and the subchondral
302 trabecular bone. Whether cartilage damage in OA affects the underlying bone or vice versa is still a
303 matter of debate. During disease progression, the structural changes in OA bone (e.g. increased
304 number of trabeculae, altered mineralization or osteophytes) are an expected consequence of
305 alterations in the cell-mediated bone remodeling process [24]. Therefore, the idea of osteoclasts
306 being directly involved in OA cartilage degradation has gained increasing attention. It is well
307 known that Peripheral Blood Mononuclear Cells (PBMCs) from OA subjects show a high
308 osteoclastogenic differentiation capability [25]. Moreover, Type A synoviocytes isolated from
309 pathological synovial membrane can differentiate into osteoclasts [26,27] and this process is
310 stimulated by M-CSF produced by type B synoviocytes.

311 The other key cellular players in bone remodeling are mesenchymal stem/stromal cells (MSCs). The
312 behavior of MSCs is linked to several factors, such as chronic inflammation and age, but the
313 underlying mechanisms and possible roles of interaction between MSCs and other specialized cells
314 remain undefined. MSCs exert their beneficial effects via secretion of bioactive molecules
315 (paracrine action), which can be antiapoptotic, mitotic, supportive for tissue resident progenitors,
316 angiogenic, immunomodulating, or chemoattractant. Moreover, they support osteoclastogenesis
317 through producing the main osteoclastogenic cytokines, RANKL, as well as osteoprotegerin (OPG),

318 a soluble member of the tumor necrosis factor receptor superfamily that acts by disrupting the
319 interaction between RANKL and RANK, thus inhibiting bone resorption. Therefore, MSCs could
320 have a dual effect, by stimulating or inhibiting osteoclastogenesis, depending on the inflammatory
321 milieu. MSCs are common residents of all joint tissues, including synovial tissue and fluid [28].
322 The exact origin of the latter is not well known, but SM is considered as the most likely one [29].
323 Conflicting results are reported regarding the isolation of functionally normal MSCs from patients
324 with OA. For instance, Scharstuhl and coworkers [30] demonstrated that the chondrogenic potential
325 of MSCs is independent of age or OA etiology, whilst the group of Murphy [31] displayed that cells
326 harvested from patients with advanced OA showed reduced proliferative and chondrogenic activity.
327 Moreover, select findings raise suspicion that systemic depletion and imbalance of MSCs may
328 contribute to OA pathophysiology.

329 Since there is not yet enough evidence to support the idea that SDSCs are involved in OA
330 pathophysiology, this phenomenon in our opinion merits further consideration. To this aim, in the
331 present study, we compared SDSCs isolated from healthy and osteoarthritic subjects in terms of
332 phenotype, morphology, gene expression and capability to induce osteoclastogenesis.

333 For the isolation of SDSCs, the same protocol developed by De Bari and coworkers was used [8].
334 Cytofluorimetric analysis for the expression pattern of the surface antigens [12] of healthy and
335 pathological SDSCs was in line with that defined by previous studies [13]. Attention was paid to the
336 comparison of the positivity for CD90 and CD105 between the two cell populations, considering
337 the close association between these superficial markers and the chondrogenic potential of SDSCs
338 [32,33]. Our results showed a high positivity for CD90 and CD105, like other studies, and the
339 absence of significant differences in the percentages of positivity between healthy and OA-derived
340 cells. Overall, these data suggest the remarkable and comparable chondrogenic differentiation
341 capability of both of healthy and osteoarthritic SDSCs. This observation was corroborated by the *in*
342 *vitro* chondrogenic differentiation test and strengthened the idea of the use of SDSCs for
343 regenerative medicine approaches [34]. An interesting aspect was the increase in positivity for

344 CD106 in SDSCs derived from OA patients. The CD106 that is specific for MSCs allow us to
345 ascertain the mesenchymal nature of the isolated cells and discriminate between type B
346 synoviocytes and SDSCs. Since proinflammatory cytokines could enhance its expression level, it
347 represents a good reflection of the endogenous inflammatory milieu to which the SDSCs derived
348 from OA subjects are exposed [35]. Even if this marker has been associated with changes in
349 osteogenic and adipogenic potentials [36,37] this was not proved by our data, which showed no
350 differences between healthy and OA-derived cells.

351 From a morphological point of view, it is interesting to note that SDSCs of healthy and OA subjects
352 share the same morphological typologies with roundish structures on the cell surface, which
353 constitute specializations associated with exocytosis [38]. The peculiar oligodendritic morphologies
354 observed in both healthy and OA cultures are suggestive for the presence of telocytes. These
355 interstitial cells, characterized by long cytoplasmic processes named telopodes and recently
356 demonstrated also in the synovial membrane [17], seem to be more numerous in culture obtained
357 from OA subjects in comparison to the healthy ones. Since TCs play an important role in many
358 pathological processes and in adaptive responses [39,40], their increased number in culture obtained
359 from OA subjects suggests their possible involvement in OA.

360 Interesting results emerged from the analysis of genes involved in bone remodeling (i.e. RANKL
361 and OPG). The comparison of their expression in cells of healthy and OA subjects showed a higher
362 RANKL/OPG ratio in SDSCs of OA subjects. This occurrence, like what observed in periosteum-
363 derived stem cells of elderly subjects [41], suggested a potential contribution of SDSCs in the
364 activation of multinucleated cells (chondroclasts and/or osteoclasts), responsible for cartilage
365 erosion or subchondral bone resorption during age-related joint diseases, such as OA. To the best
366 of our knowledge, no studies evaluated the potential of SDSCs isolated from OA, to favor the
367 differentiation of PBMCs in active osteoclasts. For this reason, we decided to deepen our
368 knowledge by evaluating the capability of SDSCs to generate active osteoclasts, by co-culturing
369 SDSCs harvested from healthy and OA synovial membranes with PBMCs from healthy donors. Our

370 trans-well approach showed the presence of paracrine signals that induced osteoclastogenesis.
371 Immunofluorescence for cytoskeleton evidenced the presence of plentiful F-actin ring positive cells
372 containing more than 3 nuclei in both samples and zipper-like structures [42], which were more
373 numerous after the induction with OA-SDSCs. Resorption assays performed on dentin slices
374 underlined that only paracrine signals derived from cells harvested by OA subjects were able to
375 determine the formation of resorption pits. The immunohistochemical analysis for Cathepsin K and
376 TRAP confirmed the differentiation of PBMCs into osteoclasts in both co-cultures and strengthened
377 SEM observations. Both osteoclast populations express cathepsin K, with a higher positivity in
378 cells stimulated by healthy SDSCs. Cathepsin K is a cysteine protease, markedly expressed in active
379 osteoclasts, whose function is the degradation of collagen type I [43]. In the ruffled border,
380 Cathepsin K can cleave the inactive form of TRAP to obtain the functionally active protein [44].
381 OCs derived from healthy SDSCs do not exhibit functional activity and, for this reason, they
382 accumulate Cathepsin K in the cytoplasmic compartment. As concern TRAP, no significant
383 differences in its expression were found between the two-different stimulations. It must be
384 underlined that this enzyme is normally released in the ruffled border as an inactive monomeric
385 form, but only the processing by Cathepsin K allow its activation and, consequently, active
386 osteoclasts.

387

388 **Conclusion**

389 In conclusion, in this study, we ascertained that SDSCs stimulated osteoclastogenesis by means of
390 soluble factors, but the osteoclast-like cells generated by healthy-SDSCs via trans-well assays, were
391 dormant. OA-derived SDSCs have much greater potency in stimulating osteoclastogenesis than
392 healthy-SDSCs. Based on our in vitro studies, it can be concluded that SDSCs have a dual effect on
393 osteoclasts, and this effect is dependent on the microenvironment. It will be also of interest confirm
394 our results with the recently developed “suspended synovium culture model” [45] to demonstrate
395 the actual role of mobilized cells.

396 Overall, these observations may represent an interesting opportunity for the development of a
397 holistic approach for OA treatment, that considers the multifaced capability of MSCs in relation to
398 the specific environment. In this respect, further studies to investigating the possible role of
399 telocytes in the onset/maintenance of the pathology as well as a new target for pharmacological
400 approaches, are desirable.

401

402 **Limitations of the study**

403 Some limitation of our study should be noted. First, only a small sample number was studied. This
404 was mainly related to the difficulties in sampling, mainly for healthy tissue. However, from each
405 explant we were capable to obtain an adequate number of cells in order to set up two different sets
406 of experiments. Moreover, no in vivo studies are included. Concerning the use of bone and joint
407 diseases model mechanism (DMM), no described indirect co-culture approaches proposed as DMM
408 for OA [46, 47] have been used, as they considered the different cell populations crosstalk. In this
409 respect our study paves the way for the development of a new in vitro DMM for OA.

410

411 **Acknowledgments**

412 The authors are grateful to Dr. Andreil Hossein for her English revision and to Dr. Sandra Manzotti
413 for her technical support. This study was funded by grants of the Università Politecnica delle
414 Marche to Prof. Monica Mattioli-Belmonte. No benefits in any form have been, or will be, received
415 from a commercial party directly, or indirectly, related to the subject of this article.

416

417

418 **Statement of author contributions:**

419 Prof. Mattioli-Belmonte planned and oversaw the whole research; Prof. Gigante furnished tissue
420 samples and clinical suggestion; Dr. Dicarlo executed cell cultures and flow cytometry study; Dr.
421 Cerqueni performed immunohistochemical analysis; Prof. Teti was responsible for ultrastructural

422 investigation; Dr. Iezzi was responsible for qRT-PCR analysis; Prof. Falconi oversaw
423 morphological analyses. All authors equally and competently contributed to the draft.

424

425

426 **References**

- 427 [1] Golightly YM, Allen KD, Jordan JM. Defining the Burden of Osteoarthritis in Population-
428 Based Surveys. *Arthritis Care Res* 2016;68:571–573. doi:10.1002/acr.22716.
- 429 [2] Li MH, Xiao R, Li JB, Zhu Q. Regenerative approaches for cartilage repair in the treatment of
430 osteoarthritis. *Osteoarthritis Cartilage* 2017;25:1577–1587. doi:10.1016/j.joca.2017.07.004.
- 431 [3] Loeser RF, Goldring SR, Scanzello CR, Goldring MB. Osteoarthritis: a disease of the joint as
432 an organ. *Arthritis Rheum* 2012;64:1697–1707. doi:10.1002/art.34453.
- 433 [4] Smith MD. The normal synovium. *Open Rheumatol J* 2011;5:100–106.
434 doi:10.2174/1874312901105010100.
- 435 [5] Bartok B, Firestein GS. Fibroblast-like synoviocytes: key effector cells in rheumatoid arthritis.
436 *Immunol Rev* 2010;233:233–255. doi:10.1111/j.0105-2896.2009.00859.x.
- 437 [6] Barland P, Novikoff AB, Hamerman D. Electron microscopy of the human synovial
438 membrane. *J Cell Biol* 1962;14:207–220.
- 439 [7] Kiener HP, Karonitsch T. The synovium as a privileged site in rheumatoid arthritis: cadherin-
440 11 as a dominant player in synovial pathology. *Best Pract Res Clin Rheumatol* 2011;25:767–
441 777. doi:10.1016/j.berh.2011.11.012.
- 442 [8] De Bari C, Dell’Accio F, Tylzanowski P, Luyten FP. Multipotent mesenchymal stem cells
443 from adult human synovial membrane. *Arthritis Rheum* 2001;44:1928–1942.
444 doi:10.1002/1529-0131(200108)44:8<1928::AID-ART331>3.0.CO;2-P.

- 445 [9] Hermida-Gómez T, Fuentes-Boquete I, Gimeno-Longas MJ, Muiños-López E, Díaz-Prado S,
446 de Toro FJ et al. Quantification of cells expressing mesenchymal stem cell markers in healthy
447 and osteoarthritic synovial membranes. *J Rheumatol* 2011;38:339–349.
448 doi:10.3899/jrheum.100614.
- 449 [10] Djouad F, Bony C, Häupl T, Uzé G, Lahlou N, Louis-Pence P, et al. Transcriptional profiles
450 discriminate bone marrow-derived and synovium-derived mesenchymal stem cells. *Arthritis*
451 *Res Ther* 2005;7:R1304-1315. doi:10.1186/ar1827.
- 452 [11] Kurth T, Hedbom E, Shintani N, Sugimoto M, Chen FH, Haspl M et al. Chondrogenic
453 potential of human synovial mesenchymal stem cells in alginate. *Osteoarthritis Cartilage*
454 2007;15:1178–1189. doi:10.1016/j.joca.2007.03.015.
- 455 [12] de Sousa EB, Casado PL, Moura Neto V, Duarte MEL, Aguiar DP. Synovial fluid and
456 synovial membrane mesenchymal stem cells: latest discoveries and therapeutic perspectives.
457 *Stem Cell Res Ther* 2014;5:112. doi:10.1186/scrt501.
- 458 [13] Sakaguchi Y, Sekiya I, Yagishita K, Muneta T. Comparison of human stem cells derived from
459 various mesenchymal tissues: superiority of synovium as a cell source. *Arthritis Rheum*
460 2005;52:2521–2529. doi:10.1002/art.21212.
- 461 [14] Mattioli-Belmonte M, Teti G, Salvatore V, Focaroli S, Orciani M, Dicarlo M, et al. Stem cell
462 origin differently affects bone tissue engineering strategies. *Front Physiol* 2015;6:266.
463 doi:10.3389/fphys.2015.00266.
- 464 [15] Kim M-J, Son MJ, Son M-Y, Seol B, Kim J, Park J, et al. Generation of human induced
465 pluripotent stem cells from osteoarthritis patient-derived synovial cells. *Arthritis Rheum*
466 2011;63:3010–3021. doi:10.1002/art.30488.

- 467 [16] Ilas DC, Churchman SM, McGonagle D, Jones E. Targeting subchondral bone mesenchymal
468 stem cell activities for intrinsic joint repair in osteoarthritis. *Future Sci OA* 2017;3:FSO228.
469 doi:10.4155/fsoa-2017-0055.
- 470 [17] Rosa I, Marini M, Guasti D, Ibba-Manneschi L, Manetti M. Morphological evidence of
471 telocytes in human synovium. *Sci Rep* 2018;8:3581. doi:10.1038/s41598-018-22067-5.
- 472 [18] Cretoiu SM, Popescu LM. Telocytes revisited. *Biomol Concepts* 2014;5:353–369.
473 doi:10.1515/bmc-2014-0029.
- 474 [19] Dominici M, Le Blanc K, Mueller I, Slaper-Cortenbach I, Marini F, Krause D et al. Minimal
475 criteria for defining multipotent mesenchymal stromal cells. The International Society for
476 Cellular Therapy position statement. *Cytotherapy* 2006;8:315–317.
477 doi:10.1080/14653240600855905.
- 478 [20] Ragni E, Viganò M, Rebullà P, Giordano R, Lazzari L. What is beyond a qRT-PCR study on
479 mesenchymal stem cell differentiation properties: how to choose the most reliable
480 housekeeping genes. *J Cell Mol Med* 2013;17:168–180. doi:10.1111/j.1582-
481 4934.2012.01660.x.
- 482 [21] Livak KJ, Schmittgen TD. Analysis of relative gene expression data using real-time
483 quantitative PCR and the $2^{-\Delta\Delta C(T)}$ Method. *Methods San Diego Calif*
484 2001;25:402–408. doi:10.1006/meth.2001.1262.
- 485 [22] Loeser RF. Aging processes and the development of osteoarthritis. *Curr Opin Rheumatol*
486 2013;25:108–113. doi:10.1097/BOR.0b013e32835a9428.
- 487 [23] Sharma AR, Jagga S, Lee S-S, Nam J-S. Interplay between cartilage and subchondral bone
488 contributing to pathogenesis of osteoarthritis. *Int J Mol Sci* 2013;14:19805–19830.
489 doi:10.3390/ijms141019805.

- 490 [24] Wong SHJ, Chiu KY, Yan CH. Review Article: Osteophytes. *J Orthop Surg Hong Kong*
491 2016;24:403–410. doi:10.1177/1602400327.
- 492 [25] Durand M, Komarova SV, Bhargava A, Trebec-Reynolds DP, Li K, Fiorino C et al.
493 Monocytes from patients with osteoarthritis display increased osteoclastogenesis and bone
494 resorption: the In Vitro Osteoclast Differentiation in Arthritis study. *Arthritis Rheum*
495 2013;65:148–158. doi:10.1002/art.37722.
- 496 [26] Danks L, Sabokbar A, Gundle R, Athanasou NA. Synovial macrophage-osteoclast
497 differentiation in inflammatory arthritis. *Ann Rheum Dis* 2002;61:916–21.
- 498 [27] Suzuki Y, Tsutsumi Y, Nakagawa M, Suzuki H, Matsushita K, Beppu M, et al. Osteoclast-like
499 cells in an in vitro model of bone destruction by rheumatoid synovium. *Rheumatol Oxf Engl*
500 2001;40:673–682.
- 501 [28] Sugita N, Moriguchi Y, Sakaue M, Hart DA, Yasui Y, Koizumi K et al. Optimization of
502 human mesenchymal stem cell isolation from synovial membrane: Implications for subsequent
503 tissue engineering effectiveness. *Regen Ther* 2016;5:79–85. doi:10.1016/j.reth.2016.09.002.
- 504 [29] Jones EA, English A, Henshaw K, Kinsey SE, Markham AF, Emery P et al. Enumeration and
505 phenotypic characterization of synovial fluid multipotential mesenchymal progenitor cells in
506 inflammatory and degenerative arthritis. *Arthritis Rheum* 2004;50:817–827.
507 doi:10.1002/art.20203.
- 508 [30] Scharstuhl A, Schewe B, Benz K, Gaissmaier C, Bühring H-J, Stoop R. Chondrogenic
509 potential of human adult mesenchymal stem cells is independent of age or osteoarthritis
510 etiology. *Stem Cells Dayt Ohio* 2007;25:3244–3251. doi:10.1634/stemcells.2007-0300.

- 511 [31] Murphy JM, Dixon K, Beck S, Fabian D, Feldman A, Barry F. Reduced chondrogenic and
512 adipogenic activity of mesenchymal stem cells from patients with advanced osteoarthritis.
513 *Arthritis Rheum* 2002;46:704–713. doi:10.1002/art.10118.
- 514 [32] Fickert S, Fiedler J, Brenner RE. Identification, quantification and isolation of mesenchymal
515 progenitor cells from osteoarthritic synovium by fluorescence automated cell sorting.
516 *Osteoarthritis Cartilage* 2003;11:790–800.
- 517 [33] Nagase T, Muneta T, Ju YJ, Hara K, Morito T, Koga H, Nimura A et al. Analysis of the
518 chondrogenic potential of human synovial stem cells according to harvest site and culture
519 parameters in knees with medial compartment osteoarthritis. *Arthritis Rheum* 2008;58:1389–
520 1398. doi:10.1002/art.23418.
- 521 [34] Wyles CC, Houdek MT, Behfar A, Sierra RJ. Mesenchymal stem cell therapy for
522 osteoarthritis: current perspectives. *Stem Cells Cloning Adv Appl* 2015;8:117–24.
523 doi:10.2147/SCCAA.S68073.
- 524 [35] Laschober GT, Brunauer R, Jamnig A, Singh S, Hafen U, Fehrer C et al. Age-specific changes
525 of mesenchymal stem cells are paralleled by upregulation of CD106 expression as a response
526 to an inflammatory environment. *Rejuvenation Res* 2011;14:119–131.
527 doi:10.1089/rej.2010.1077.
- 528 [36] Fukiage K, Aoyama T, Shibata KR, Otsuka S, Furu M, Kohno Y et al. Expression of vascular
529 cell adhesion molecule-1 indicates the differentiation potential of human bone marrow stromal
530 cells. *Biochem Biophys Res Commun* 2008;365:406–412. doi:10.1016/j.bbrc.2007.10.149.
- 531 [37] Liu F, Akiyama Y, Tai S, Maruyama K, Kawaguchi Y, Muramatsu K, Yamaguchi K. Changes
532 in the expression of CD106, osteogenic genes, and transcription factors involved in the

- 533 osteogenic differentiation of human bone marrow mesenchymal stem cells. *J Bone Miner*
534 *Metab* 2008;26:312–320. doi:10.1007/s00774-007-0842-0.
- 535 [38] Vandenameele F, De Bari C, Moreels M, Lambrechts I, Dell'Accio F, Lippens PL.
536 Morphological and immunocytochemical characterization of cultured fibroblast-like cells
537 derived from adult human synovial membrane. *Arch Histol Cytol* 2003;66:145–153.
- 538 [39] Ardeleanu C, Bussolati G. Telocytes are the common cell of origin of both PEComas and
539 GISTs: an evidence-supported hypothesis. *J Cell Mol Med* 2011;15:2569–2574.
540 doi:10.1111/j.1582-4934.2011.01461.x.
- 541 [40] Niculite CM, Regalia TM, Gherghiceanu M, Huica R, Surcel M, Ursaciuc C et al. Dynamics
542 of telopodes (telocyte prolongations) in cell culture depends on extracellular matrix protein.
543 *Mol Cell Biochem* 2015;398:157–164. doi:10.1007/s11010-014-2215-z.
- 544 [41] Ferretti C, Lucarini G, Andreoni C, Salvolini E, Bianchi N, Vozzi G et al. Human Periosteal
545 Derived Stem Cell Potential: The Impact of age. *Stem Cell Rev* 2015;11:487–500.
546 doi:10.1007/s12015-014-9559-3.
- 547 [42] Takito J, Nakamura M, Yoda M, Tohmonda T, Uchikawa S, Horiuchi K et al. The transient
548 appearance of zipper-like actin superstructures during the fusion of osteoclasts. *J Cell Sci*
549 2012;125:662–672. doi:10.1242/jcs.090886.
- 550 [43] Costa AG, Cusano NE, Silva BC, Cremers S, Bilezikian JP. Cathepsin K: its skeletal actions
551 and role as a therapeutic target in osteoporosis. *Nat Rev Rheumatol* 2011;7:447–456.
552 doi:10.1038/nrrheum.2011.77.
- 553 [44] Ljusberg J, Wang Y, Lång P, Norgård M, Dodds R, Hultenby K et al. Proteolytic excision of a
554 repressive loop domain in tartrate-resistant acid phosphatase by cathepsin K in osteoclasts. *J*
555 *Biol Chem* 2005;280:28370–28381. doi:10.1074/jbc.M502469200.

- 556 [45] Katagiri K, Matsukura Y, Muneta T, Ozeki N, Mizuno M, Katano H et al. Fibrous Synovium
557 Releases Higher Numbers of Mesenchymal Stem Cells Than Adipose Synovium in a
558 Suspended Synovium Culture Model. *Arthroscopy* 2016; 33: 800 - 810
559 doi.org:10.1016/j.arthro.2016.09.033
- 560 [46] Sanchez C, Deberg MA, Piccardi N, Msika P, Reginster JY, Henrotin YE. Subchondral bone
561 osteoblasts induce phenotypic changes in human osteoarthritic chondrocytes. *Osteoarthritis*
562 *Cartilage* 2005;11:988-97. DOI:10.1016/j.joca.2005.07.012
- 563 [47] Van Buul GM, Villafuertes E, Bos PK, Waarsing JH, Kops N, Narcisi R et al. Mesenchymal
564 stem cells secrete factors that inhibit inflammatory processes in short-term osteoarthritic
565 synovium and cartilage explant culture. *Osteoarthritis Cartilage*. 2012;10:1186-96. DOI:
566 10.1016/j.joca.2012.06.003.

567

568 **Figure legends:**

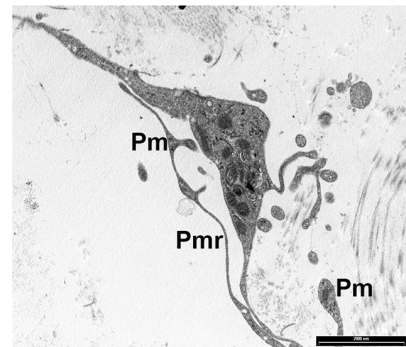
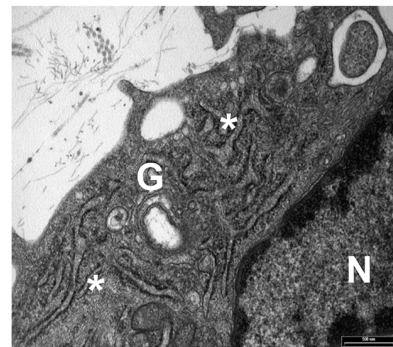
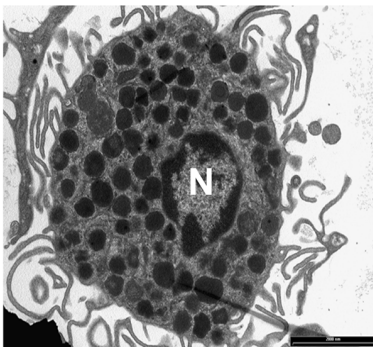
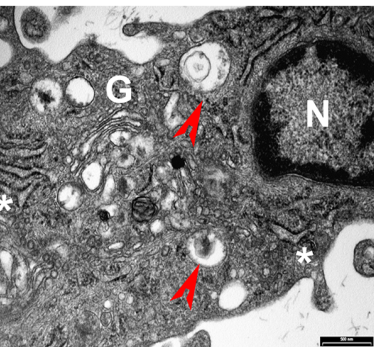
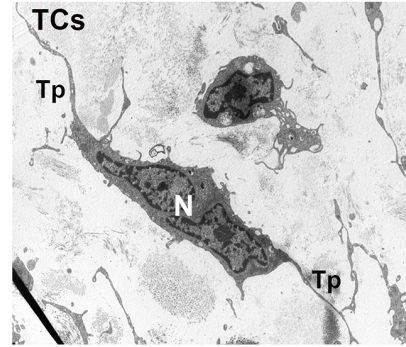
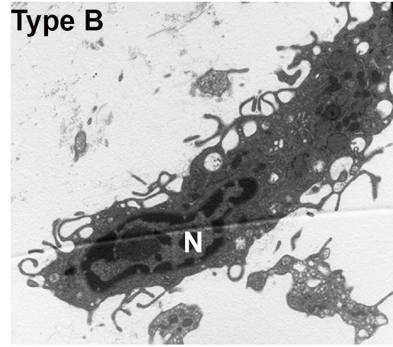
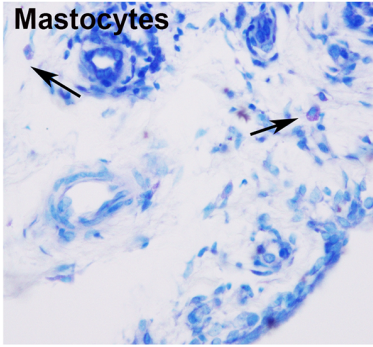
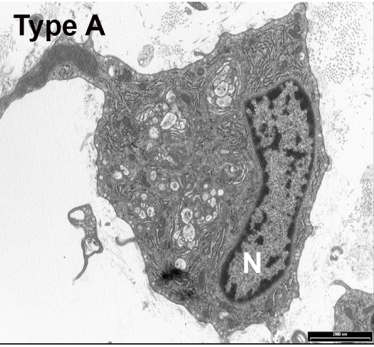
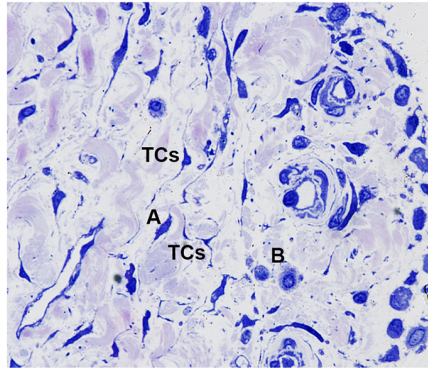
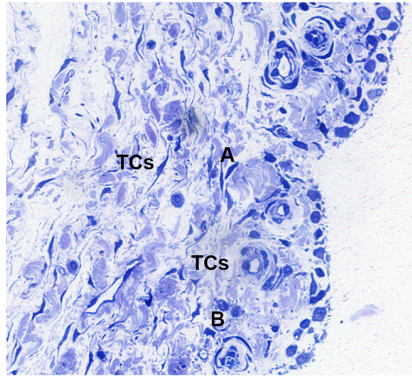
569

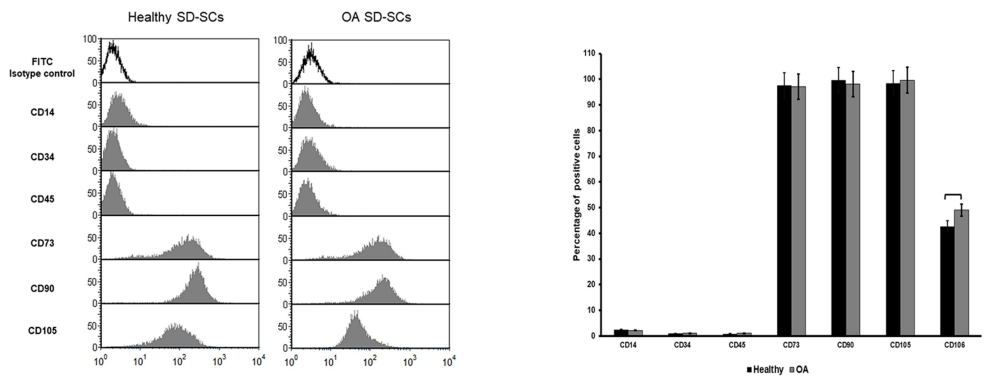
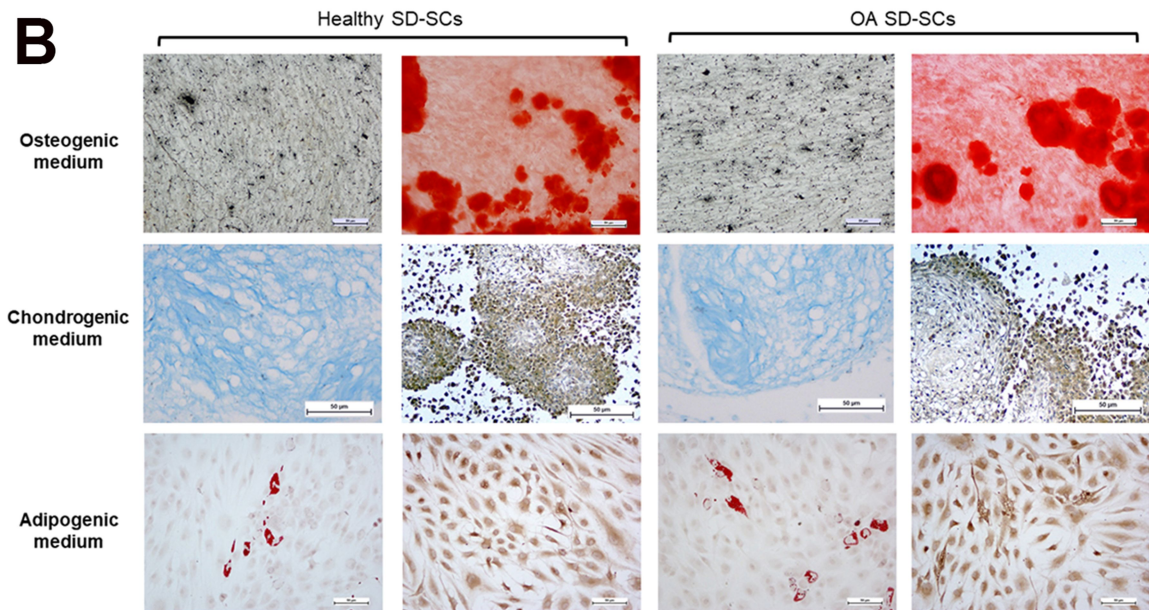
570 **Figure 1:** Representative semithin section of OA-SM. Types A and B synoviocytes as well as
571 telocytes (TCs) are detectable. TEM morphological images of Types A and B synoviocytes,
572 mastocytes and TCs present in OA -SM. N=Nucleus; G=Golgi apparatus; TP= telopodes;
573 Pm=podomes; Pmr= podomers; Red arrows indicate lysosomes; Asterisks indicate rough
574 endoplasmic reticulum.

575 **Figure 2:** A) Cytofluorimetric analysis of the detection of MSC surface markers in SDSCs isolated
576 from Healthy and OA-SM (white plots indicate FITC negative controls), square brackets indicate
577 significant ($p < 0.05$) differences; B) Differentiation of SDSCs isolated from Healthy and OA-SM
578 towards osteoblasts (Von Kossa and Alizarin red stainings; scale bars: 50 μ m), chondrocytes
579 (Alcian blue staining and IHC for aggrecan; scale bars: 50 μ m) and adipocytes (Oil red staining and

580 IHC for perilipin; scale bars: 10 μ m); C) SEM and TEM representative images of cells isolated from
581 Healthy and OA-SM; TCs=telocytes; Tp= telopodes.

582 **Figure 3:** A) Representative images displaying the generation of osteoclast-like cells after coculture
583 of Healthy- or OA-SDSCs with normal PBMCs: Immunofluorescence for actin evidenced the
584 appearance of the actin ring and of zipper-like structures (arrow); SEM observation on dentin slices
585 were consistent with active osteoclast-like in OA-SDSCs/PBMCs co-culture; B) IHC detection of
586 cathepsin K (CTK) and TRAP in Osteoclast-like cells after 14 days of co- culture with Healthy- or
587 OA-SDSCs, square brackets indicate significative ($p<0.05$) differences; C) Histograms depict
588 changes in mRNA expression of genes involved in bone remodelling (Opg and RANKL) in
589 Healthy- or OA-SDSCs, data are expressed as Fold-regulation ($2^{-\Delta\Delta Ct}$) (see Material and
590 Methods); D) Histogram depicts changes in RANKL/OPG ratio in Healthy- or OA-SDSCs before
591 and after co-culture. Scale bars: 50 μ m; square brackets indicate significative ($p<0.05$) differences.



A**B****C**